Water Science & Technology

Water Science & Technology Vol 90 No 3, 995 doi: 10.2166/wst.2024.267

Spatial differences of dissolved organic matter composition and humification in an artificial lake

Jin Zhang[a,*], Jiajia Tan[b] and Yingjie Wang[c]

[a] School of Environmental and Chemical Engineering, Shanghai University, Shanghai, 200444, China
[b] Zhejiang Environmental Monitoring Engineering Co., Ltd, Hangzhou, 310000, China
[c] Zhejiang Environmental Research Institute Co., Ltd, Hangzhou, 310000, China
*Corresponding author. E-mail: zhangj@shu.edu.cn

ABSTRACT

The depth-dependent dynamics of dissolved organic matter (DOM) structure and humification in an artificial lake limits the understanding of lake eutrophication and carbon cycling. Using fluorescence regional integration (FRI) and parallel factor analysis (PARAFAC) models to analyze the 3D fluorescence spectroscopy dataset, we revealed the depth-dependent structure and vertical distribution of DOM in the estuarine and center regions of Lake Hongfeng. The percentage fluorescence response ($P_{i,n}$) showed humic acid is an important part of DOM in Lake Hongfeng. Fluorescence results show that the fulvic-like and protein-like materials in HF1-DOM located at the estuarine position showed greater variation in the middle stage, probably due to human influence and sediment suspension. Fluorescence index ($P_{I+II+IV,n}/P_{III+V,n}$ and FI_{C4}/FI_{C3}) can be used to indicate the degree of humification of DOM in artificial lakes. Results of each index show that the estuary is more affected by human activities, and the humification degree is significantly lower than that of the center of the lake. The evaluation index system of the humification degree of artificial lake established in this study can effectively predict the eutrophication state of the typical area of artificial lake and deeply understand the possible important influence of human activities on the carbon cycle of lake.

Key words: artificial lake, dissolved organic matter, fluorescence indices, humification degree, parallel factor analysis

HIGHLIGHTS

- Complex factors in the estuary of the lake lead to significant changes in DOM structure.
- Depth-dependent change sensitivity was for humic > fulvic> protein-like components.
- Higher DOM humification in the middle of the lake is attributed to microbial action.
- Spectral indices were confirmed to evaluate the DOM humification degree.

GRAPHICAL ABSTRACT

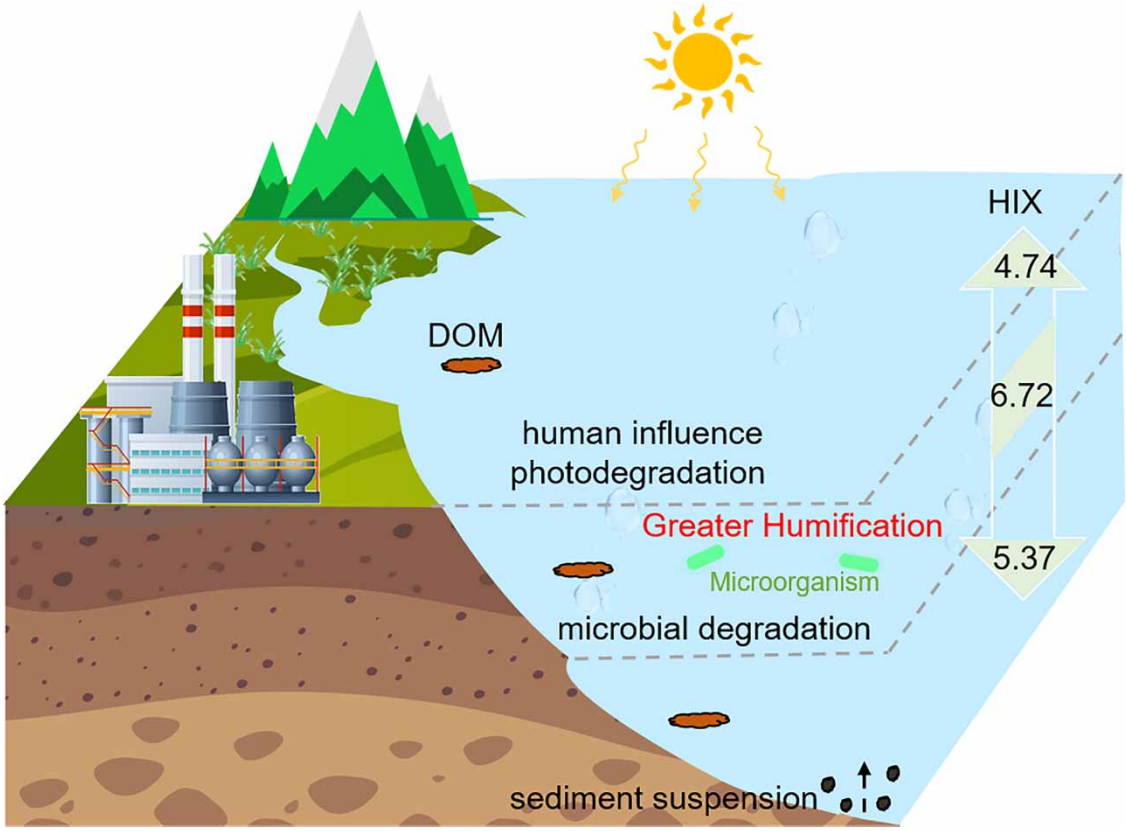

1. INTRODUCTION

In recent years, there has been a gradual increase in the impact of human activities and climate change on the eutrophication of lakes, such that these impacts can lead to the accumulation of dissolved organic carbon (DOC) (Liu *et al.* 2021; Li *et al.* 2022; Nai *et al.* 2023). The spatial and temporal dynamic distribution of DOC in lakes has an extremely complex impact on the lake carbon cycle and is currently at the forefront of lake carbon cycle research (Liu *et al.* 2022). Dissolved organic matter (DOM), as a complex heterogeneous complex (Jeong & Kwak 2021; Huang *et al.* 2022), is used as a good tracer of DOC sources in lakes (Wickland *et al.* 2007). Most of the current studies have focused on the distribution of DOM in plateau lakes (Song *et al.* 2019), freshwater lakes (Huang *et al.* 2022), and saltwater lakes (Du *et al.* 2016), while there is a relative lack of studies on the vertical dynamic distribution of DOM composition structure and degree of humification in artificial lakes (which are most affected by human activities). According to previous studies (Liu *et al.* 2020; Ke *et al.* 2023), the composition and structure of DOM show large variations by various human activities. Therefore, elucidating the effects of depth variation in artificial lakes on the composition structure and degree of humification of DOM is of great scientific significance for an in-depth understanding of lake eutrophication and carbon cycling.

Estuaries connect lake–lake, lake–river (Zhou *et al.* 2019), and lake–ocean ecosystems and are key areas of the global carbon cycle (He *et al.* 2022). These ecosystems are significantly affected by human activities, estuarine circulation is driven by vertical and lateral advection, and spatial and temporal changes in the phytoplankton community structure and biomass due to discharge currents (Geyer & MacCready 2014; Zhou *et al.* 2021; Perrot *et al.* 2023; Phlips *et al.* 2023). Estuaries can bring a large amount of DOM into the lake, making the source of DOM at different depths in the lake estuary, and the composition varies greatly (Jaffé *et al.* 2004). The estuarine environment is subject to natural and anthropogenic influences and the re-suspension of sediments into the lake (Harfmann *et al.* 2021), the further release of DOM from the sediment into the lake makes the differences further significant. However, these differences also limit the understanding

of lake eutrophication and carbon cycling. Therefore, revealing the dynamic patterns of DOM composition and humification with depth in artificial lake estuaries is a primary task in assessing lake eutrophication and carbon cycling.

Three-dimensional excitation–emission matrix fluorescence spectroscopy (3D EEM) is a technique widely used to characterize the fluorescent properties of DOM (Coble 1996; Wufuer *et al.* 2014; Yuan *et al.* 2023). However, due to the complexity and heterogeneity of DOM compositions, overlapping fluorescence spectroscopy cannot be identified accurately in 3D EEM (Song *et al.* 2018). The 3D EEM combined with fluorescence regional integration (3D EEM-FRI) can be used to determine the integration of the volume below each region of the 3D EEM in the DOM and quantify the fluorescence intensity (FI) in the specified region (Hua *et al.* 2007; Wu *et al.* 2011; Song *et al.* 2017). Additionally, the 3D EEM coupling with parallel factor analysis (3D EEM-PARAFAC) has the advantage of decomposing the fluorescence signal of DOM into relatively independent fluorescent components to reduce the interference between fluorescent components (Chen *et al.* 2003; Zhang *et al.* 2011; Sgroi *et al.* 2017; Zhao *et al.* 2017). Both 3D EEM-FRI and 3D EEM-PARAFAC have been applied widely to analyze 3D EEM spectral characteristics of DOM from aquatic environments (Chen *et al.* 2003; Du *et al.* 2016; Song *et al.* 2019). Therefore, both 3D EEM-FRI and 3D EEM-PARAFAC can be applied to analyze the dynamics of DOM composition structure with depth in the estuary of an artificial lake. Biological index (BIX) and humification index (HIX) are powerful fluorescence indices, and are commonly used to investigate the source of DOM and the degree of humification (Du *et al.* 2021). The values of HIX and BIX suggested that Lakes-Yangtze River DOM was dominated by freshly-generated compounds with low terrestrial humic contents (Du *et al.* 2021). Therefore, the combination of the 3D EEM-FRI/PARAFAC method and fluorescence indices will support the chemical characteristics (e.g. degree of humification) and the vertical distribution characteristics of the constituents of DOM in the artificial lake estuary, and construct a fluorescence index system to predict the degree of humification of DOM in the artificial lake estuary, providing theoretical support for understanding eutrophication and carbon cycling in the artificial lake estuary.

In this study, Lake Hongfeng, the largest artificial lake in Guizhou Province, was selected as the subject. 3D EEM, FRI/PARAFAC and fluorescence indexes were used to study the spatial distribution of DOM structure in the lake. The objectives were as follows: (1) to study the vertical changes of fluorescence components and humification degree of DOM in estuarine and lake center; (2) to study the vertical variation of DOM fluorescence index; (3) develop and propose a new method for evaluating the humification degree of DOM based on fluorescence index.

2. MATERIALS AND METHODS

2.1. Sample collection

Lake Hongfeng is a typical artificial lake in the upper and middle of the Maotiao River, a first-level tributary of the Wujiang River in Guizhou plateau, China. With a lake surface area of 57.2 km^2 and a water retention time of 0.325 years, the lake provides multiple services including irrigation, aquaculture, functioning as a drinking water source, and improving peripheral ecosystems (Supplementary material, Figure S1) (Wang *et al.* 2009). Water samples were collected in March 2023 from the estuary (marked as HF-1) and centre (marked as HF-2) of Lake Hongfeng (Supplementary material, Figure S1). The 24 samples were collected from HF1 with depths of 0, 1, 3, 5, 7, 9, 11, 13, 15, 17, and 19 m, and from HF-2 with depths of 0, 2, 4, 6, 8, 10, 12, 14, 16, 18, 20, 22 and 24 m, respectively. All water samples were stored in plastic bottles in the dark at 4 °C. All water samples were transported to the laboratory and filtered through 0.45 μm glass fiber filters (pre-combusted at 450 °C for 6 h) within 10 h. The pH and DOC of all collected samples ranged from 6.8 to 7.8 and 1.3–2.1 mg/L, respectively.

2.2. 3D EEM measurement

The 3D EEMs of DOM were obtained with the emission wavelength (Em) from 250 to 500 nm with 2 nm increments, and the Ex from 220 to 400 nm with 5 nm increments using a fluorescence spectrometer (Hitachi F-4500, Japan). The slit widths for Em and Ex were 10 and 5 nm, respectively. The scanning speed and PMT voltage were set at 1,200 nm·min^{-1} and 400 V, respectively. The inner filter effects were established by diluting the Lake Hongfeng with pure water (Milli-Q, 18.2 MΩcm), and the inner correction was unnecessary for our samples based on UV-Vis absorbance (Guo *et al.* 2015). The inner effects of DOM were also ignored during the investigation of natural lake waters, and sea waters, as well as simulating water with fulvic acids and humic acid with low concentration of DOM (Guo *et al.* 2015).

2.3. 3D EEM-FRI analysis

According to 3D EEM-FRI theory (Chen *et al.* 2002). The percentage of fluorescence response ($P_{i,n}$) for each region can be expressed as Equation (1).

$$P_{i,n} = \frac{\Phi_{i,n}}{\Phi_{t,n}} \times 100\% = \frac{\mathrm{MF}_i \sum \mathrm{Ex} \sum \mathrm{Em} I(\mathrm{ExEm}) \Delta\mathrm{Ex}\Delta\mathrm{Em}}{\sum_{i=1}^{5} \Phi_{i,n}} \times 100\%, \quad i = I - V \tag{1}$$

where, $\phi_{i,n}$ and $\phi_{t,n}$ are the Ex/Em area volumes that involve the value of region i and the total region t, respectively. MF_i is the multiplication factor for each region. I(ExEm) is the fluorescence intensity at the wavelength Ex and wavelength Em. ΔEx and ΔEm are the Ex and Em increments, respectively. FRI analysis was performed using MATLAB 2009 (MathWorks, Inc., USA).

2.4. 3D EEM-PARAFAC analysis

Combining 3D EEM and PARAFAC (3D EEM-PARAFAC), an interactive least squares algorithm can be used to decompose a ternary array into residual arrays and trilinear terms. The PARAFAC analysis could be described by Equation (2).

$$x_{hjk} = \sum_{m=1}^{M} a_{hf} b_{jf} c_{kf} + \varepsilon_{hjk}, h = 1, \ldots, H;\ j = 1, \ldots, J;\ k = 1, \ldots, K \tag{2}$$

where, x_{hjk} is the fluorescence intensity for the hth sample at Em j and Ex k. The a_{hf} is directly proportional to the concentration (defined as scores) of fluorophore component f in sample h. Both b_{jf} and c_{kf} are estimated values of the wavelength Em and wavelength Ex for the fluorophore component f (defined as loadings), respectively. ε_{hjk} is the residual noise, representing the variability unexplained by the model (He *et al.* 2013; Maqbool & Hur 2016; Song *et al.* 2017). M is the amount of fluorophore components in the samples.

The possible effects of Rayleigh and Raman scatters were minimized with two steps. First, subtracting the 3D EEMs of Milli-Q water from each 3D EEM of solution samples. Second, the area without fluorescence (Em $<<$Ex) is inserted as a series of zero values (Bahram *et al.* 2006). The 2–7 component models that based on PARAFAC, using residual analysis and half-split analysis to determine the appropriate number of PARAFAC components in DOM. The maximum FI of PARAFAC components was used to represent the concentration of the PARAFAC component (Bahram *et al.* 2006; Guo *et al.* 2015). The 3D EEM-PARAFAC was performed by use of MATLAB 2009a (MathWorks, Inc., USA) with drEEM toolbox (www.models.life.ku.dk). The Pearson correlation analysis and principal component analysis (PCA) for $P_{i,n}$, FI, HIX and BIX of DOM were also calculated using SPSS 16.0 software.

3. RESULTS AND DISCUSSION

Each original 3D EEM exhibited two main peaks and a shoulder peak for both HF1-DOM and HF2-DOM named Peak A (located at Ex/Em 225–235/425–445 nm), Peak B (located at Ex/Em 305–320/420–445 nm), respectively (Figure 1). Peaks A and peak B were related to fulvic- and humic-like materials, respectively. Peak A and B with similar locations were also reported during the investigation of DOM in Suwannee River and Black Sea (Chen *et al.* 2003; Coble 1996). The intensities of Peaks A and B were observed as the change of depths (Figure 1). In detail, the intensities of Peak A-B of HF1-DOM exhibited the greater FI at the depth of 9 m as the depth increased (from 0 to 19 m), indicating that the DOM content in the estuary was more in the middle layer. The intensities of Peaks A-B of HF2-DOM exhibited greater FI at the depth of 24 m as the depth increased (from 0 to 24 m), indicating that the DOM content in the center of the lake was more in the bottom position. The regional heterogeneity of DOM structure further indicates that it is necessary to study the spatial changes of DOM structure in artificial lakes.

3.1. 3D EEM-FRI analysis of DOM in different water depths

Based on the FRI theory, five regions in the 3D EEMs of the DOM from different sources represent the following Regions I (Ex/Em: 220–250/250–330 nm) and II (Ex/Em: 220–250/330–380 nm), region III (Ex/Em: 220–250/380–500 nm), region IV (Ex/Em: 250–400/250–380 nm), region V (Ex/Em: 250–400/380–500 nm) (Chen *et al.* 2003). Peaks A and B are located in Region III and Region V, respectively (Figure 1, Supplementary material, Table S1). Regions III, V, and II were represented as

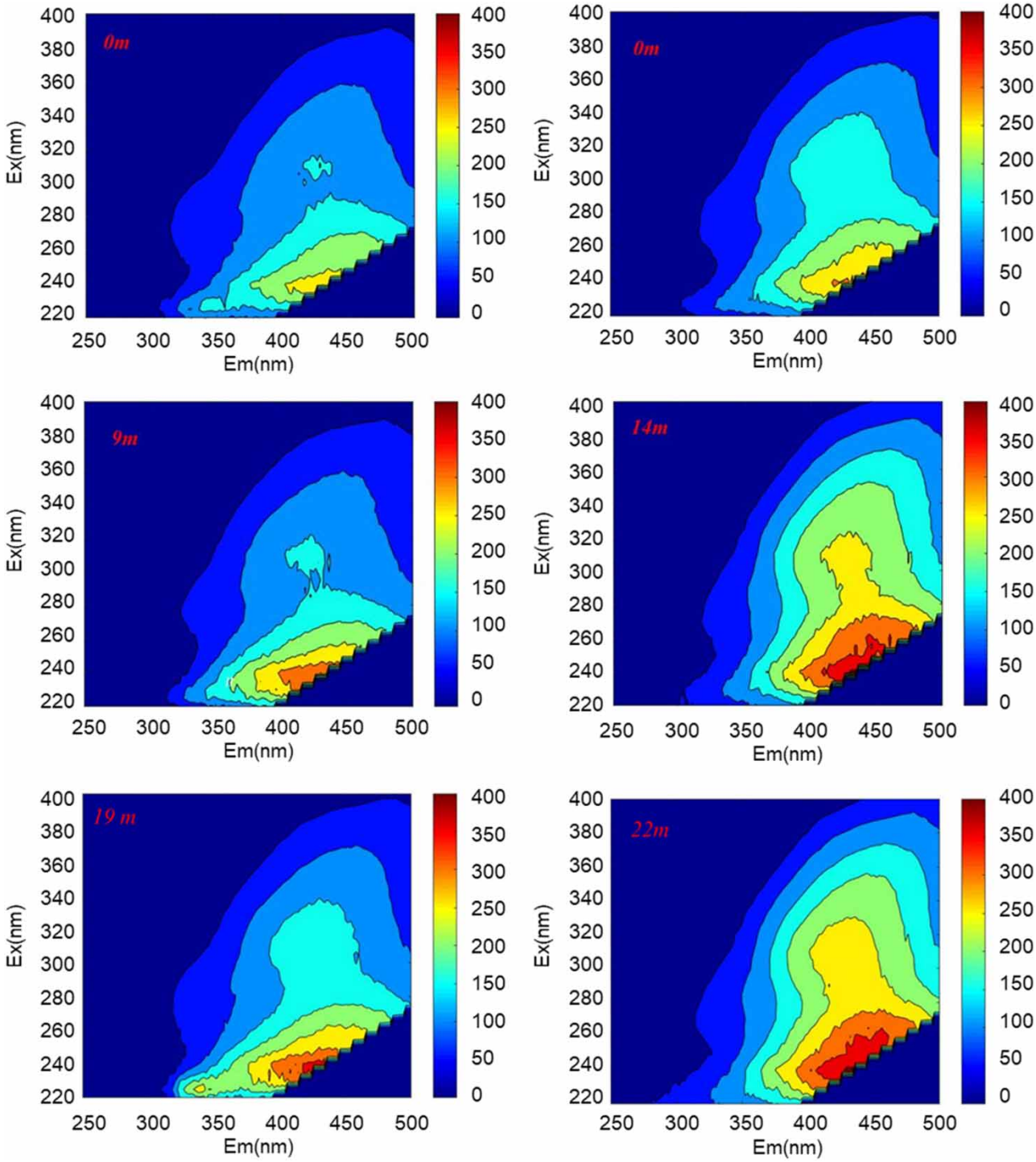

Figure 1 | 3D EEMs of HF1-DOM (left) and HF2-DOM (right) with depth in Lake Hongfeng. Color bar represents the intensity of fluorescence.

fulvic- and humic-like materials (Figure 1, Supplementary material, Table S1). This result was consistent with the 3D EEM categorization results above.

The values of $P_{i,n}$ are shown in Supplementary material, Figure S2. The fluorescent materials measured in HF1-DOM and HF2-DOM, in descending order of content, were humic-like materials > fulvic-like materials > protein-like materials. The ratio of humic-like ($P_{V,n}$) : fulvic-like ($P_{III,n}$) : tyrosine-like ($P_{I,n}$ and $P_{II,n}$) : tryptophan-like ($P_{IV,n}$) materials is about

12:4:2:1 according to 3D EEM-FRI analysis of both HF1-DOM and HF2-DOM. In detail, the $P_{V,n}$ values of the DOM were the greatest at 61.1 ± 1.1% and 65.8 ± 1.2% for HF-1 (HF1-DOM) and HF-2 (HF2-DOM), respectively, indicating that humic-like materials were the primary fluorescent components in Lake Hongfeng (Supplementary material, Figure S2). Fulvic-like materials ($P_{III,n}$) accounted 22.2 ± 1.0% and 20.1 ± 0.3% for HF1-DOM and HF2-DOM, respectively (Supplementary material, Figure S2). Tyrosine-like materials ($P_{I,n}$ and $P_{II,n}$) accounted 9.9 ± 0.5% and 9.1 ± 0.6% for HF1-DOM and HF2-DOM, respectively (Supplementary material, Figure S2). Tryptophan-like materials ($P_{IV,n}$) accounted for 6.8 ± 0.6% and 5.1 ± 0.3% for HF1-DOM and HF2-DOM, respectively (Supplementary material, Figure S2). Tryptophan- and tyrosine-like materials were classified as protein-like materials (Song *et al.* 2019). The consistency of the DOM composition ratio between the estuarine and lake center can prove the similarity of DOM composition in the whole region of Lake Hongfeng.

3.2. The 3D EEM-PARAFAC analysis of DOM in different water depths

The optimum number of fluorescent components in the DOM was 4 identified according to split analysis and residual analysis of PARAFAC analysis for 24 samples of DOM. These were denoted Component 1 (C1) at Ex/Em (250–265) 345–360/455–475 nm and Component 2 (C2) at Ex/Em 225–240/410–425 nm (Figure 2 and Table 1). C1 and C2 represented the humic-like components (Chen *et al.* 2003). Both C1 and C2 with similar locations in 3D EEM were also reported during the investigation of DOM in lakes, rivers and seas (Zhang *et al.* 2011; Song *et al.* 2017), which might be produced of terrestrial organic matter or those derived from the degradation of organic substances such as terrestrial plants or microbes (Chen *et al.* 2003). As two kinds of humic-like components, the Em wavelength of C1 was approximately 45–50 nm longer than that of C2, indicating that C1 of the DOM consisted of more conjugated π-electron systems with electron-withdrawing substituents than C2 (Chen *et al.* 2002). Even though C1 and C2 are the same substance, they still have slight structural differences. Component 3 (C3) at Ex/Em (220–235) 275–290/335–350 nm and Component 4 (C4) at Ex/Em (230–245) 305–320/395–405 nm. The C3 and C4 represented the protein- and fulvic-like components (Zhang *et al.* 2011; Du *et al.* 2016; Song *et al.* 2017), respectively (Figure 2, Table 1).

The values of FI are shown in Figure 2, the order of the content of the fluorescent components was as follows: humic-like components (262.78 a.u.) > fulvic-like components (182.80 a.u.) > protein-like components (113.66 a.u.), which was consistent with the $P_{i,n}$ values results of FRI analysis for both HF1-DOM and HF2-DOM. Three stages including surface (0–4 m), middle (4–12 m), and bottom (12–24 m) stages were observed for FI of C1-C4 for both HF1-DOM and HF2-DOM with lake depth, as determined using the 3D EEM-PARAFAC method (Figure 3). For the surface and bottom stages, no significant changes (<10%) were found in the FI values of C1-C4 in HF1-DOM and HF2-DOM (Figure 3), indicating that the composition of HF1-DOM and HF2-DOM was stable in surface and bottom of Lake Hongfeng. This phenomenon might be due to the fact that both HF1-DOM and HF2-DOM were affected by photodegradation and biodegradation (Song *et al.* 2019). Interestingly, for the stage at the mid-level, the change of variation of FI for HF1-DOM was larger than that of HF2-DOM (Figure 3), indicating that the composition of HF1-DOM varied significantly more than HF2-DOM in the mid-level of Lake Hongfeng.

3.3. Analysis of the biological and humification indices of DOM

The BIX and HIX were used to assess the differences in the sources and degrees of humification of DOM in the water ecosystem (Birdwell & Engel 2010; Xiao *et al.* 2016). According to the previous study (Zhou *et al.* 2021), the $0.6 < BIX < 0.8$, indicated that the DOM has strong terrestrial characteristics (Helms *et al.* 2013). The HIX > 6 showed relatively strong terrestrial and humification characteristics (Zhang *et al.* 2010). Figure 4 shows the vertical distribution of HIX and BIX values with depth in Lake Hongfeng. The values of HIX indicated that the DOM had weak autogenic characteristics at the depth of 0–7 m (4.74–5.81), and strong terrestrial and humification characteristics (6.04–6.72) at the depth of 9–19 m for HF1-DOM. The values of HIX indicated that the DOM had weak autogenic characteristics at the depth of 0–14 m (5.37–6.00), and strong terrestrial and humification characteristics (6.23–7.02) at the depth of 14–22 m for HF2-DOM. The greatest HIX values were obtained for HF1-DOM (6.72) and HF2-DOM (7.02) at depths of 9 and 14 m, respectively (Figure 4), indicating that humification was stronger at depths of 9–14 m in Lake Hongfeng. Interestingly, the value of HIX in HF2-DOM (6.23–7.02) was higher than HF1-DOM (6.17–6.72) at depths of 9–14 m, indicating that humification was stronger at depths of 9–14 m in HF2. The stronger humification was likely to relate to the microbial and non-biological stable degradation of DOM (Song *et al.* 2019).

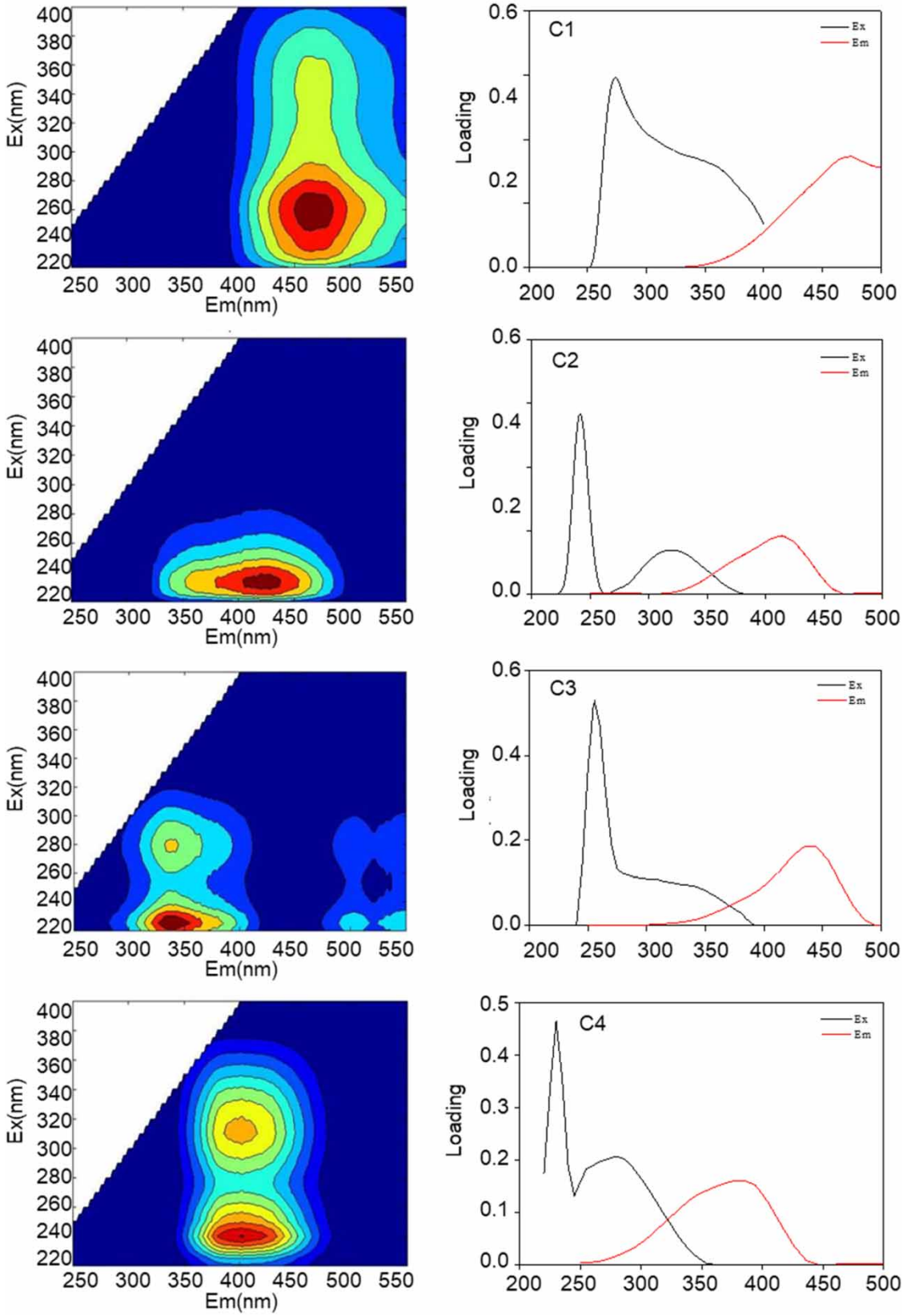

Figure 2 | Identified PARAFAC components (C1-C4) of DOM of Lake Hongfeng with arbitrary unit. C1 refers to humic-like components, C2 refers to humic-like components, C3 refers to protein-like components, C4 refers to fulvic-like components.

Table 1 | Locations and categories of PARAFAC components of DOM in Lake Hongfeng

	C1			C3		C4	
Components	**First**	**Second**	**C2**	**First**	**Second**	**First**	**Second**
Position (nm)	Ex : 250–265 Em: 455–475	Ex: 345–360 Em: 455–475	Ex: 225–240 Em: 410–425	Ex: 220–235 Em: 335–350	Ex: 275–290 Em: 335–350	Ex: 230–245 Em: 395–405	Ex: 305–320 Em: 395–405
Components categories	Humic-like		Humic-like	Protein-like		Fulvic-like	

C1–C4 were the components of DOM distinguished by 3D EEM combined with the PARAFAC method. FI refers to maximum fluorescence intensity.

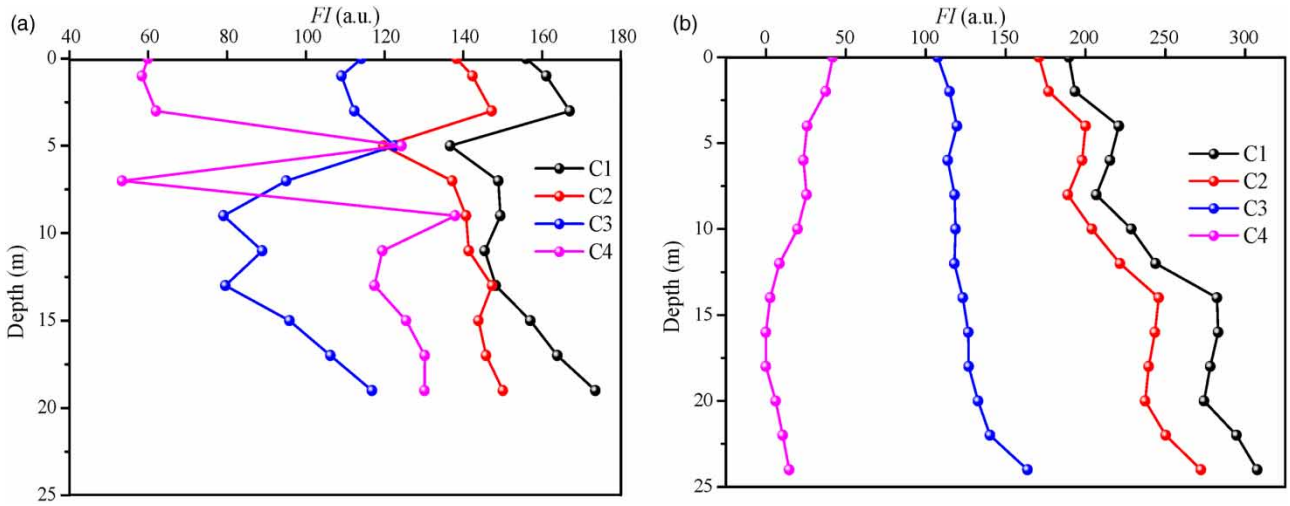

Figure 3 | Values of FI of HF1-DOM (a) and HF2-DOM (b) with water depth in Lake Hongfeng. C1-C4 were the components of DOM distinguished by 3D EEM combined with PARAFAC method. FI, maximum fluorescence intensity.

Overall, the HF1-DOM located in the estuarine position contains higher levels of protein-like materials (16.7%) than the HF2-DOM (14.2%), indicating a greater human influence on the composition of the DOM at the estuarine location. This result is consistent with those obtained in previous studies (Du *et al.* 2021; He *et al.* 2022). The most significant variation with depth in protein-like and fulvic acid-like fractions (>50%) was found in HF1-DOM at the estuarine location, likely due to human influence and sediment suspension in this area (Zhou *et al.* 2018; Harfmann *et al.* 2021). The large difference between the HIX of the middle layer of HF1-DOM (1.35) and that of the surface layer and the middle layer further indicates that the unstable water conditions at the estuary lead to an unstable microbial degradation process, resulting in DOM stratification. Additionally, a previous study found that vertical and lateral advection significantly contributes to the stratification of the water column at estuarine locations (Geyer & MacCready 2014; Zhou *et al.* 2021; Perrot *et al.* 2023; Phlips *et al.* 2023). This natural phenomenon may also play a role in DOM stratification.

3.4. Correlation analysis of the DOM fluorescence indices

Significant positively linear corrections ($r = 0.992$, $p < 0.01$) was observed for FI_{C1} vs. FI_{C4}, whereas the negatively significant correlations were exhibited between FI_{C3} vs. FI_{C4} ($r = -0.680$, $p < 0.01$) and FI_{C2} vs. FI_{C4} ($r = -0.851$, $p < 0.01$), respectively (Supplementary material, Figure S3a–3c, Table 2). The PARAFAC components representing different sources may exhibit significant correlations, especially protein-like components that are more relevant to human activity inputs (Song *et al.* 2019). In addition, the greater positive significant correlations of FI_{C4} vs. FI_{C1} ($r = 0.992$, $p < 0.01$) suggested that the humic-like components containing more conjugated π-electron systems with electron-withdrawing substituents and fulvic-like components in DOM might have the same source of origin. However, the greater negative significant correlations of FI_{C4} vs. FI_{C2} ($r = -0.851$, $p < 0.01$) suggested that the humic-like components containing less carboxylic-like and phenolic-like groups

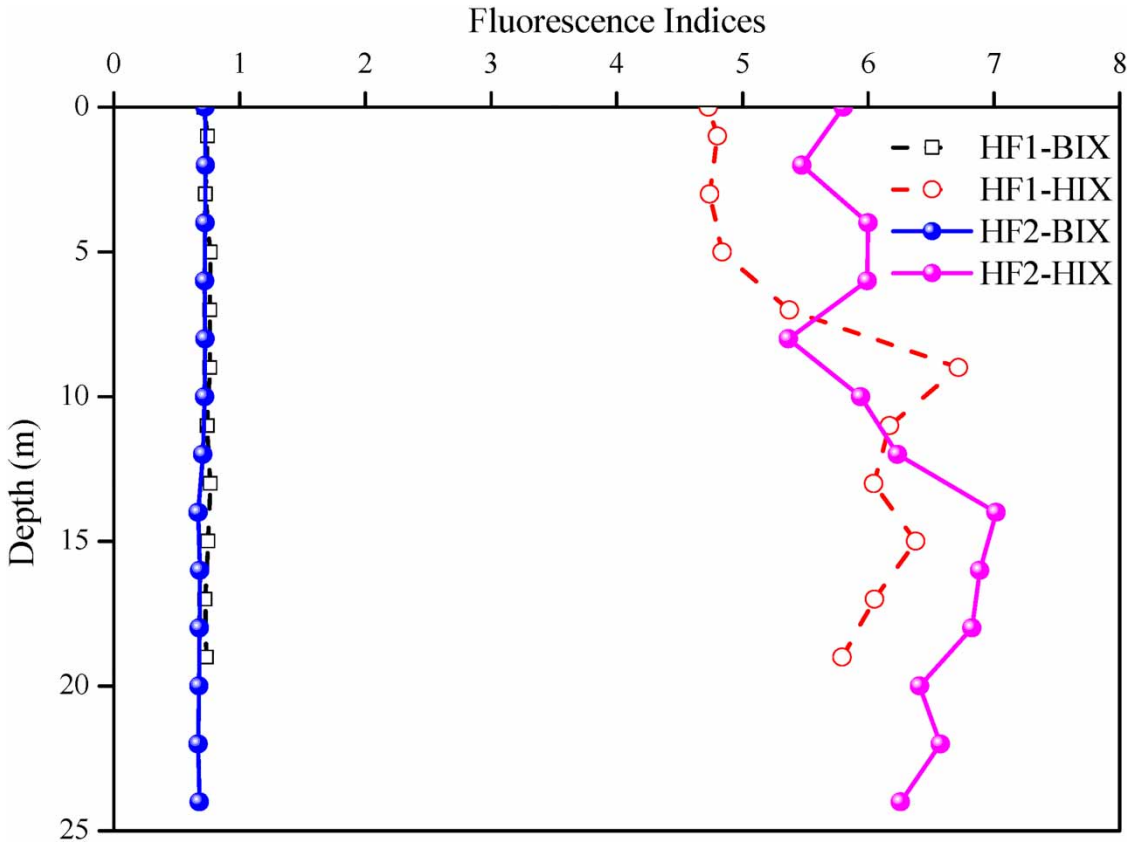

Figure 4 | HIX and BIX values of DOM with water depth. The dotted lines and solid lines represented HF-1 and HF-2, respectively.

and fulvic-like components in DOM might have a different source of origin. The different correlations shown by FI_{C1} and FI_{C2} with FI_{C4} also support PARAFAC's analysis of subtle structural differences in the same components. The significant correlations of humic- and fulvic-like components suggested might have the same source of region reported by Song *et al.*, who studied depth-dependent of DOM in Lake Baihua using fluorescence spectroscopy (Song *et al.* 2019).

The correlation analyses of the fluorescence indices were summarized for DOM in Lake Hongfeng (Figure 5(a), 5(b), Table 2). Previous research documented that the sum of the percent fluorescence responses of 3D EEM Regions I, II, and IV ($P_{I+II+IV,n}$) had related to biochemical characteristics of DOM (Bilal *et al.* 2010). Meanwhile, the sum of the percent fluorescence responses of 3D EEM Regions III and V ($P_{III+V,n}$) showed the geochemical characteristics of DOM (Bilal *et al.* 2010). For the DOM in Lake Hongfeng, the $P_{I+II+IV,n}/P_{III+V,n}$ values were within the ranges of 0.15–0.23. The BIX was found to be positively correlated with $P_{I+II+IV,n}/P_{III+V,n}$ ($r = 0.854$, $p < 0.01$) (Table 2). The BIX have negatively correlated with FI of C1 (FI_{C1}) ($r = -0.926$, $p < 0.01$), FI of C4 (FI_{C4}) ($r = -0.894$, $p < 0.01$), and the ratio of fulvic-like to humic-like ($FI_{C4}/(FI_{C1} + FI_{C2})$) ($r = -0.734$, $p < 0.01$) (Table 2). These results show that the fluorescence indices $P_{I+II+IV,n}/P_{III+V,n}$, FI_{C1}, FI_{C4}, and $FI_{C4}/(FI_{C1} + FI_{C2})$ can be used to indicate the relative contribution of autogenic organic matter to DOM.

The HIX was negatively correlated with BIX ($r = -0.598$, $p < 0.01$) and $P_{I+II+IV,n}/P_{III+V,n}$ ($r = -0.720$, $p < 0.01$), and positively correlated with FI_{C1} ($r = 0.576$, $p < 0.01$), FI_{C4} ($r = 0.584$, $p < 0.01$), and the radio of fulvic-like to protein-like components (FI_{C4}/FI_{C3}) ($r = 0.772$, $p < 0.01$) (Table 2). There were no significant correlations between HIX and FI_{C2} and FI_{C3}. That is, the degree of humification of the DOM decreased as the increase of the values of BIX and $P_{I+II+IV,n}/P_{III+V,n}$, as well as the decrease of the values of FI_{C1}, FI_{C4}, and FI_{C4}/FI_{C3}. The fluorescence indices $P_{I+II+IV,n}/P_{III+V,n}$, FI_{C1}, FI_{C4}, and FI_{C4}/FI_{C3} can be used to indicate the degree of humification of DOM in artificial lakes. Furthermore, the minimum $P_{I+II+IV,n}/P_{III+V,n}$ value (0.15–0.2) and the maximum FI_{C4}/FI_{C3} value (1.59–2.00) occurred at the depths of 9 and 14 m showed the least content of protein-like component and the highest humification level of DOM, which is consistent with the results of the HIX analysis.

Table 2 | Pearson correlation analysis for fluorescence indices of DOM

	$P_{I,n}/P_{II,n}$	$P_{I+II+IV,n}/P_{III+V,n}$	FI_{C4}/FI_{C3}	$FI_{C4}/(FI_{C1}+FI_{C2})$	$FI_{C3}/(FI_{C1}+FI_{C2})$	BIX	HIX	FI_{C1}	FI_{C2}	FI_{C3}	FI_{C4}
$P_{I,n}/P_{II,n}$	1	−0.723**	0.479*	0.953**	0.851**	−0.684**	0.085	0.807**	−0.971**	0.743**	0.811**
$P_{I+II+IV,n}/P_{III+V,n}$		1	−0.872**	−0.857**	−0.298	0.854**	−0.720**	−0.925**	0.817**	−0.558**	−0.938**
FI_{C4}/FI_{C3}			1	0.684**	−0.025	−0.575**	0.772**	0.682**	−0.600**	0.164	0.737**
$FI_{C4}/(FI_{C1}+FI_{C2})$				1	0.704**	−0.734**	0.311	0.860**	−0.984**	0.657**	0.833**
$FI_{C3}/(FI_{C1}+FI_{C2})$					1	−0.390	−0.376	0.486*	−0.765*	0.709**	0.472**
BIX						1	−0.598**	−0.926**	−0.748**	0.750**	−0.894**
HIX							1	0.576**	−0.241	0.130	0.584**
FI_{C1}								1	−0.854**	0.819**	0.992**
FI_{C2}									1	0.785**	−0.851**
FI_{C3}										1	−0.680**
FI_{C4}										-	1

FI refers to maximum fluorescence intensity.

**Correlation is highly significant at the 0.01 level (two-tailed).

*Correlation is significant at the 0.05 level (two-tailed).

'–' represents negatively correlation.

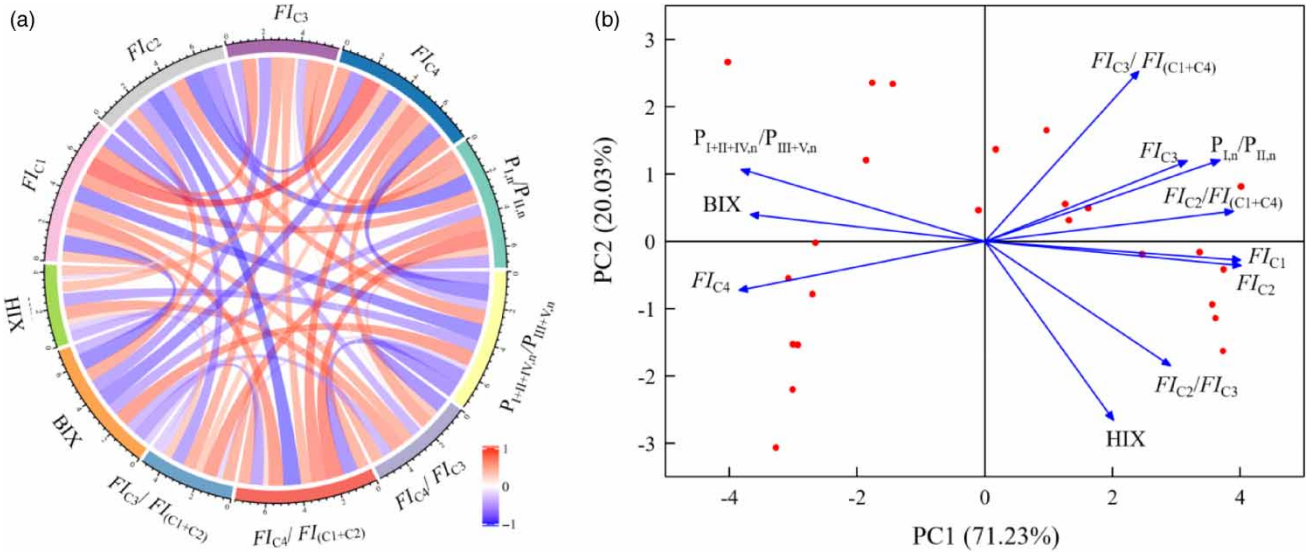

Figure 5 | Circular correlation chord diagram (a) and PCA analysis (b) based on the various fluorescence indices.

PCA was performed on the fluorescence indices of the DOM (Figure 5(b)). The principal components PC1 and PC2 had variance contributions of 71.23% and 20.03%, respectively. The greater sum of variance contributions (91.26%) indicated that PC1 and PC2 could be used to reflect the degree of humification and the influence of human activities on Lake Hongfeng, respectively. The fluorescence indices including HIX and FI_{C4}/FI_{C3} related to fulvic-like and humic-like materials had large positive loadings with PC1, indicating that PC1 could be presented as the degree of humification. The greater values of HIX and FI_{C4}/FI_{C3} indicated the greater content of humic-like and fulvic-like materials, as well as the greater degree of humification in Lake Hongfeng. The fluorescence indices including BIX and $P_{I+II+IV,n}/P_{III+V,n}$ related to protein-like materials presented the large positive loadings of PC2 according to PCA analysis (Figure 5(b)), indicated that PC2 could present the influence of human activities. The fluorescence indices $P_{I+II+IV,n}/P_{III+V,n}$ and FI_{C4}/FI_{C3} can be used to indicate the degree of humification and the influence of human activities of DOM in artificial lakes. From the perspective of Lake Hongfeng as a whole, the humification degree of the middle water is higher and the influence of human activities is lower. More importantly, the low $P_{I+II+IV,n}/P_{III+V,n}$ and FI_{C4}/FI_{C3} values of the estuarine also indicate that the water body in the estuarine has a low degree of humification and is greatly affected by human activities.

Characterizing changes in the composition and humification of DOM with depth in estuaries of artificial lakes can aid in assessing water quality and predicting the fate of various pollutants in aquatic systems. Moreover, the combined multi-fluorescence indices of DOM can be utilized to respond to sudden water quality deterioration, design water supply system intakes, and manage the sustainability of water ecosystems. Understanding depth-dependent changes in DOM will provide valuable insights for water quality assessment and contamination risk prediction at different depths in estuaries.

4. CONCLUSIONS

Based on 3D EEM-FRI, the composition of DOM in Lake Hongfeng is consistent and not affected by the region where it is located. Humic acid is an important part of DOM in Lake Hongfeng. Changes in the composition of HF1-DOM and HF2-DOM with increasing lake depth were observed in three stages, including surface, middle, and bottom stages. The composition of HF1-DOM and HF2-DOM did not change significantly in both the surface and bottom stages, whereas the composition of HF1-DOM located at the estuarine location varied more in the middle stage with no obvious pattern, probably due to the estuarine location being subject to human influence and sediment suspension. The BIX (0.67–0.77) and HIX (4.74–7.02) indicated that the DOM had relatively weak autogenic characteristics in the surface stage and relatively strong terrestrial characteristics in the middle and bottom stages. The HIX had negatively correlated with $P_{I+II+IV,n}/P_{III+V,n}$ ($r = -0.720$, $p < 0.01$), and positively correlated with FI_{C2}/FI_{C3} ($r = 0.772$, $p < 0.01$), indicating that $P_{I+II+IV,n}/P_{III+V,n}$ and FI_{C4}/FI_{C3} can be used to indicate the degree of humification of DOM in artificial lake. The results of each index show that the middle water

body of Lake Hongfeng is less affected by human activities, the estuary is more affected by human activities, and the humification degree is significantly lower than that of the center of the lake. It is noteworthy that in terms of quantifying the uncertainty in optical changes, the variations in DOM are primarily concentrated in the fluorescence component. More advanced techniques are required to quantify changes in the molecular structure of DOM, rather than simply making direct comparisons of fluorescence changes. Despite the need to consider certain finer limitations and uncertainties, the multi-indicator coupled assessment system for the degree of humification in artificial lakes established by this study will significantly enhance our understanding of the biogeochemical processes in artificial lake systems.

ACKNOWLEDGEMENT

This work was supported jointly by the Shanghai Post-doctoral Excellence Program (2023331).

DATA AVAILABILITY STATEMENT

All relevant data are included in the paper or its Supplementary Information.

CONFLICT OF INTEREST

The authors declare there is no conflict.

REFERENCES

Bahram, M., Bro, R., Stedmon, C. & Afkhami, A. 2006 Handling of Rayleigh and Raman scatter for PARAFAC modeling of fluorescence data using interpolation. *Journal of Chemometrics* **20** (3–4), 99–105.

Bilal, M., Jaffrezic, A., Dudal, Y., Le Guillou, C., Menasseri, S. & Walter, C. 2010 Discrimination of farm waste contamination by fluorescence spectroscopy coupled with multivariate analysis during a biodegradation study. *Journal of Agricultural and Food Chemistry* **58** (5), 3093–3100.

Birdwell, J. E. & Engel, A. S. 2010 Characterization of dissolved organic matter in cave and spring waters using UV–Vis absorbance and fluorescence spectroscopy. *Organic Geochemistry* **41** (3), 270–280.

Chen, J., Gu, B. H., LeBoeuf, E. J., Pan, H. J. & Dai, S. 2002 Spectroscopic characterization of the structural and functional properties of natural organic matter fractions. *Chemosphere* **48**, 59–68.

Chen, W., Westerhoff, P., Leenheer, J. A. & Booksh, K. 2003 Fluorescence excitation – Emission matrix regional integration to quantify spectra for dissolved organic matter. *Environmental Science & Technology* **24**, 5701–5710.

Coble, P. G. 1996 Characterization of marine and terrestrial DOM in seawater using excitation-emission matrix spectroscopy. *Marine Chemistry* **51**, 325–346.

Du, Y., Zhang, Y., Chen, F., Chang, Y. & Liu, Z. 2016 Photochemical reactivities of dissolved organic matter (DOM) in a sub-alpine lake revealed by EEM-PARAFAC: An insight into the fate of allochthonous DOM in alpine lakes affected by climate change. *Science of The Total Environment* **568**, 216–225.

Du, Y., Lu, Y., Roebuck Jr., J. A., Liu, D., Chen, F., Zeng, Q., Xiao, K., He, H., Liu, Z., Zhang, Y. & Jaffe, R. 2021 Direct versus indirect effects of human activities on dissolved organic matter in highly impacted lakes. *Science of The Total Environment* **752**, 141839.

Geyer, W. R. & MacCready, P. 2014 The estuarine circulation. *Annual Review of Fluid Mechanics* **46**, 175–197.

Guo, X. J., Zhu, N.-m., Chen, L., Yuan, D.-h. & He, L.-s. 2015 Characterizing the fluorescent properties and copper complexation of dissolved organic matter in saline-alkali soils using fluorescence excitation-emission matrix and parallel factor analysis. *Journal of Soils and Sediments* **15** (7), 1473–1482.

Harfmann, J. L., Avery, G. B., Rainey, H. D., Mead, R. N., Skrabal, S. A., Kieber, R. J., Felix, J. D., Helms, J. R. & Podgorski, D. C. 2021 Composition and lability of photochemically released dissolved organic matter from resuspended estuarine sediments. *Organic Geochemistry* **151**, 104164.

He, X. S., Xi, B. D., Li, X., Pan, H. W., An, D., Bai, S. G., Li, D. & Cui, D. Y. 2013 Fluorescence excitation-emission matrix spectra coupled with parallel factor and regional integration analysis to characterize organic matter humification. *Chemosphere* **93** (9), 2208–2215.

He, D., Li, P., He, C., Wang, Y. & Shi, Q. 2022 Eutrophication and watershed characteristics shape changes in dissolved organic matter chemistry along two river-estuarine transects. *Water Research* **214**, 118196.

Helms, J. R., Stubbins, A., Perdue, E. M., Green, N. W., Chen, H. & Mopper, K. 2013 Photochemical bleaching of oceanic dissolved organic matter and its effect on absorption spectral slope and fluorescence. *Marine Chemistry* **155**, 81–91.

Hua, B., Dolan, F., McGhee, C., Clevenger, T. E. & Deng, B. 2007 Water-source characterization and classification with fluorescence EEM spectroscopy: PARAFAC analysis. *International Journal of Environmental Analytical Chemistry* **87** (2), 135–147.

Huang, Q., Liu, L., Huang, J., Chi, D., Devlin, A. T. & Wu, H. 2022 Seasonal dynamics of chromophoric dissolved organic matter in Poyang Lake, the largest freshwater lake in China. *Journal of Hydrology* **605**, 127298.

Jaffé, R., Boyer, J. N., Lu, X., Maie, N., Yang, C., Scully, N. M. & Mock, S. 2004 Source characterization of dissolved organic matter in a subtropical mangrove-dominated estuary by fluorescence analysis. *Marine Chemistry* **84** (3–4), 195–210.

Jeong, Y.-H. & Kwak, D.-H. 2021 Factors affecting behavior and distribution of dissolved organic matter in an artificial coastal reservoir. *Regional Studies in Marine Science* **44**, 101786.

Ke, Z., Tang, J., Yang, L., Sun, J. & Xu, Y. 2023 Linking pharmaceutical residues to dissolved organic matter and aquatic bacterial communities in a highly urbanized bay. *Science of The Total Environment* **871**, 162027.

Li, S., Fang, J., Zhu, X., Spencer, R. G. M., Alvarez-Salgado, X. A., Deng, Y., Huang, T., Yang, H. & Huang, C. 2022 Properties of sediment dissolved organic matter respond to eutrophication and interact with bacterial communities in a plateau lake. *Environmental Pollution* **301**, 118996.

Liu, D., Du, Y., Yu, S., Luo, J. & Duan, H. 2020 Human activities determine quantity and composition of dissolved organic matter in lakes along the Yangtze River. *Water Research* **168**, 115132.

Liu, D., Yu, S., Xiao, Q., Qi, T. & Duan, H. 2021 Satellite estimation of dissolved organic carbon in eutrophic Lake Taihu, China. *Remote Sensing of Environment* **264**, 112572.

Liu, S., Hou, J., Suo, C., Chen, J., Liu, X., Fu, R. & Wu, F. 2022 Molecular-level composition of dissolved organic matter in distinct trophic states in Chinese lakes: Implications for eutrophic lake management and the global carbon cycle. *Water Research* **217**, 118438.

Maqbool, T. & Hur, J. 2016 Changes in fluorescent dissolved organic matter upon interaction with anionic surfactant as revealed by EEM-PARAFAC and two dimensional correlation spectroscopy. *Chemosphere* **161**, 190–199.

Nai, H., Zhong, J., Yi, Y., Lai, M., He, D., Dittmar, T., Liu, C. Q., Li, S. L. & Xu, S. 2023 Anthropogenic disturbance stimulates the export of dissolved organic carbon to rivers on the Tibetan Plateau. *Environmental Science & Technology* **57** (25), 9214–9223.

Perrot, V., Ma, T., Vandeputte, D., Smolikova, V., Bratkic, A., Leermakers, M., Baeyens, W. & Gao, Y. 2023 Origin and partitioning of mercury in the polluted Scheldt Estuary and adjacent coastal zone. *Science of The Total Environment* **878**, 163019.

Phlips, E. J., Badylak, S., Mathews, A. L., Milbrandt, E. C., Montefiore, L. R., Morrison, E. S., Nelson, N. & Stelling, B. 2023 Algal blooms in a river-dominated estuary and nearshore region of Florida, USA: The influence of regulated discharges from water control structures on hydrologic and nutrient conditions. *Hydrobiologia* **850** (20), 4385–4411.

Sgroi, M., Roccaro, P., Korshin, G. V., Greco, V., Sciuto, S., Anumol, T., Snyder, S. A. & Vagliasindi, F. G. A. 2017 Use of fluorescence EEM to monitor the removal of emerging contaminants in full scale wastewater treatment plants. *Journal of Hazardous Materials* **323**, 367–376.

Song, F., Wu, F., Guo, F., Wang, H., Feng, W., Zhou, M., Deng, Y., Bai, Y., Xing, B. & Giesy, J. P. 2017 Interactions between stepwise-eluted sub-fractions of fulvic acids and protons revealed by fluorescence titration combined with EEM-PARAFAC. *Science of The Total Environment* **605**, 58–65.

Song, F., Wu, F., Feng, W., Tang, Z., Giesy, J. P., Guo, F., Shi, D., Liu, X., Qin, N., Xing, B. & Bai, Y. 2018 Fluorescence regional integration and differential fluorescence spectroscopy for analysis of structural characteristics and proton binding properties of fulvic acid sub-fractions. *Journal of Environmental Sciences* **74**, 116–125.

Song, F., Wu, F., Feng, W., Liu, S., He, J., Li, T., Zhang, J., Wu, A., Amarasiriwardena, D., Xing, B. & Bai, Y. 2019 Depth-dependent variations of dissolved organic matter composition and humification in a plateau lake using fluorescence spectroscopy. *Chemosphere* **225**, 507–516.

Wang, L., Wu, F., Zhang, R., Li, W. & Liao, H. 2009 Characterization of dissolved organic matter fractions from Lake Hongfeng, Southwestern China Plateau. *Journal of Environmental Sciences* **21** (5), 581–588.

Wickland, K. P., Neff, J. C. & Aiken, G. R. 2007 Dissolved organic carbon in Alaskan Boreal Forest: Sources, chemical characteristics, and biodegradability. *Ecosystems* **10** (8), 1323–1340.

Wu, J., Zhang, H., He, P. J. & Shao, L. M. 2011 Insight into the heavy metal binding potential of dissolved organic matter in MSW leachate using EEM quenching combined with PARAFAC analysis. *Water Research* **45**, 1711–1719.

Wufuer, R., Liu, Y., Mu, S., Song, W., Yang, X., Zhang, D. & Pan, X. 2014 Interaction of dissolved organic matter with Hg(II) along salinity gradient in Boston Lake. *Geochemistry International* **52** (12), 1072–1077.

Xiao, K., Sun, J. Y., Shen, Y. X., Liang, S., Liang, P., Wang, X. M. & Huang, X. 2016 Fluorescence properties of dissolved organic matter as a function of hydrophobicity and molecular weight: Case studies from two membrane bioreactors and an oxidation ditch. *RSC Advances* **6**, 24050–24059.

Yuan, K., Wan, Q., Chai, B., Lei, X., Kang, A., Chen, J., Chen, X., Shi, H., He, L. & Li, M. 2023 Characterizing the effects of stormwater runoff on dissolved organic matter in an urban river (Jiujiang, Jiangxi province, China) using spectral analysis. *Environmental Science and Pollution Research* **30** (17), 50649–50660.

Zhang, Y., Zhang, E., Yin, Y., van Dijk, M. A., Feng, L., Shi, Z., Liu, M. & Qina, B. 2010 Characteristics and sources of chromophoric dissolved organic matter in lakes of the Yungui Plateau, China, differing in trophic state and altitude. *Limnology and Oceanography* **55** (6), 2645–2659.

Zhang, Y., Yin, Y., Feng, L., Zhu, G., Shi, Z., Liu, X. & Zhang, Y. 2011 Characterizing chromophoric dissolved organic matter in Lake Tianmuhu and its catchment basin using excitation-emission matrix fluorescence and parallel factor analysis. *Water Research* **45** (16), 5110–5122.

Zhao, Y., Wei, Y., Zhang, Y., Wen, X., Xi, B., Zhao, X., Zhang, X. & Wei, Z. 2017 Roles of composts in soil based on the assessment of humification degree of fulvic acids. *Ecological Indicators* **72**, 473–480.

Zhou, Y., Xiao, Q., Yao, X., Zhang, Y., Zhang, M., Shi, K., Lee, X., Podgorski, D. C., Qin, B., Spencer, R. G. M. & Jeppesen, E. 2018 Accumulation of terrestrial dissolved organic matter potentially enhances dissolved methane levels in Eutrophic Lake Taihu, China. *Environmental Science & Technology* **52** (18), 10297–10306.

Zhou, Y., Xu, X., Han, R., Li, L., Feng, Y., Yeerken, S., Song, K. & Wang, Q. 2019 Suspended particles potentially enhance nitrous oxide (N2O) emissions in the oxic estuarine waters of eutrophic lakes: Field and experimental evidence. *Environmental Pollution* **252**, 1225–1234.

Zhou, Y., He, D., He, C., Li, P., Fan, D., Wang, A., Zhang, K., Chen, B., Zhao, C., Wang, Y., Shi, Q. & Sun, Y. 2021 Spatial changes in molecular composition of dissolved organic matter in the Yangtze River Estuary: Implications for the seaward transport of estuarine DOM. *Science of The Total Environment* **759**, 143531.

First received 25 March 2024; accepted in revised form 12 July 2024. Available online 2 August 2024